

RESEARCH ARTICLE

Investigation of the Electrical Properties of PAN-GO/p-Si Schottky Diode

Haluk Koralay¹  • Yusuf Öznal²  • Selçuk İzmirli³  • Neslihan Turan¹ 
 • Şükrü Çavdar^{1*} 

¹Gazi University, Faculty of Science, Department of Physics, Ankara/Türkiye²Gazi University, Graduate School of Natural and Applied Sciences, Department of Physics, Ankara/Türkiye³Gazi University, Graduate School of Natural and Applied Sciences, Department of Advanced Technologies, Ankara/Türkiye

ARTICLE INFO

Article History

Received: 06.12.2022

Accepted: 19.12.2022

First Published: 21.12.2022

Keywords

Graphene oxide

Norde function

Polyacrylonitrile

Schottky diode



ABSTRACT

In this article, the electrical properties of PAN-GO/p-Si Schottky diode were investigated in the dark at room temperature. Field-emission scanning electron microscopy (FE-SEM) was utilized to study the structure of the PAN:GO interfacial layer. Diode parameters were calculated according to thermionic emission theory. By using the I-V characteristic of the prepared PAN-GO diode, the ideality factor (n), barrier height (Φ_B) and series resistance (R_s) values were evaluated with the I-V method and Norde functions. The barrier height values calculated with the I-V and Norde function were found to be 0.767 eV and 0.761 eV, respectively. The ideality factor was found to be 2.078 from the I-V method. The series resistance value of the diode was calculated as 42 k Ω using Norde functions. Energy-dependence profile of interface state density was determined from the current-voltage characteristics by considering the voltage-dependence of barrier height and ideality factor. The interface state density (N_{ss}) values of the PAN-GO/p-Si Schottky diode are $9.5 \times 10^{11} \text{ eV}^{-1} \text{ cm}^{-2}$ for 0.35-E_v eV and $1.03 \times 10^{11} \text{ eV}^{-1} \text{ cm}^{-2}$ for 0.74-E_v eV. Experimental results approved that the PAN-GO interfacial layer improved the performance of metal-semiconductor Schottky diode in respect of low ideality factor, interface state density, and high barrier height and rectification rate.

Please cite this paper as follows:

Koralay, H., Öznal, Y., İzmirli, S., Turan, N., & Çavdar, Ş. (2022). Investigation of the electrical properties of PAN-GO/p-Si Schottky diode. *Journal of Advanced Applied Sciences*, 1(1), 32-39. <https://doi.org/10.29329/jaasci.2022.476.05>

Introduction

Schottky diodes in metal-insulator-semiconductor (MIS) structure have an important place in today's technology, especially in integrated devices. These diodes are commonly used in electronic systems and optoelectronic applications such as solar cells, photo detectors, gas sensors, transistors, and switching circuits (Wang et al., 1998; Kang et al., 2016; Kumar et al., 2017; Aldirmaz et al., 2018; Al-Ahmadi, 2020; Aftab et al., 2021; Zhang et al., 2021; Aldirmaz et al., 2022; Yıldırım et al., 2022). The electrical parameters of diodes in electronic circuits are necessary for the analysis and design of the circuit. The electrical behavior of the Schottky diode is determined by

calculating parameters such as the ideality factor, barrier height, series resistance, and saturation current (I_0). To examine the Schottky diode parameters, it is possible to gain information about the diode by analyzing the current-voltage (I-V) properties (Tatar et al., 2009; Güllü & Türüt, 2010; Saloma et al., 2020). With this analysis, it becomes clear how the interface states of the MIS structure and how the transmission mechanism behaves. Using the current-voltage (I-V) data obtained using the forward bias applied to the Schottky diode, many methods have developed such as Norde, Cheng, and thermionic emission theory (Gholami et al., 2009; Gupta et al., 2009; Mahala et al., 2018). The most widely used of these calculation methods is the TE method. The diode parameters

* Corresponding author
 E-mail address: cavdar@gazi.edu.tr

are calculated using linear region of $\ln I$ - V curve. The series resistance effect in the diode structure is evaluated using all $\ln I$ - V data according to the Norde method (Norde, 1979). This method, which is valid for an ideal Schottky diode, has been generalized by Bohlin (1986) for non-ideal Schottky diode structures.

Graphene, which consists of a two-dimensional hexagonal layer of carbon atoms, is used in various applications in different fields owing to its large surface area. In electrical studies, graphene is an attractive material because it is compatible with thin-film processing. Graphene oxide (GO), a graphene-based material, attracts scientists' attention due to its high specific surface area, thermal properties and high flexibility (Kedambaimoole et al., 2020), which make it a two-dimensional support material to host metallic nanoparticles. GO is water soluble, hydrophilic, chemically stable, and mechanically resistant (Suk et al., 2010). However, unlike graphene, graphene oxide contains structural defects and covalent bond defects and is atomically rough because of this property (Vacchi et al., 2017). It is low cost and abundant because it is obtained from inexpensive graphite. It can be used in biological applications due to its excellent aqueous workability (Sun et al., 2018). This property allows it to form heterojunction devices with various semiconductors. It is also a candidate material for various applications such as gas sensing, cancer therapy, supercapacitors, field effect transistor (FET), solar cells, chemical sensors (Jaworski et al., 2015; Muazim & Hussain, 2017; Tian et al., 2019; Hue et al., 2020; Eswaran et al., 2022; Ferrag et al., 2022; Strimaitis et al., 2022; Lv et al., 2023). Polyacrylonitrile (PAN) polymer is frequently used in the preparation of nanofibers due to its water-resistance properties and can be applied in many fields such as water treatment, filtration, or medical fields (Nataraj et al., 2012). Additionally, PAN is frequently used in the production of carbon nanofibers because it has a high carbon yield (Saufi & Ismail, 2002; Lu et al., 2004). Furthermore, carbon nanofiber mats are easy to use and overcome all major challenges in dispersion, processing and transport compared to other carbon nanomaterials such as carbon nanotubes. Therefore, polyacrylonitrile polymer was chosen for the preparing Al/PAN-GO/p-Si/Al device structure. In recent years, to improve the performance or quality of MS diodes, metal-insulator-semiconductor (MIS) diodes have been changed by metal-polymer-semiconductor (MPS)-type diodes. It is known that the interface materials such as polymer or doped polymer can be commonly used in optoelectronic and electronic device. PAN-GO has advantages of both PAN and GO materials. The interface layer such as PAN-GO is a significant factor for the high performance of MIS devices. Our aim is to compose MPS type Al/PAN-GO/p-Si diodes instead of MIS type diodes due to easily growing the interfacial organic/polymer layer by spin coating between semiconductor and metal.

The aim is to produce a new type of Schottky diode using PAN-GO interfacial layer, and to determine the diode parameters by using I - V measurement. For this, Al/PAN-GO/p-Si/Al was produced using the drop casting technique. I - V measurement was performed between ± 4 V bias range in the dark at room temperature, and n , Φ_B , N_{ss} , and R_s values were calculated.

Materials and Methods

The wafer used for the PAN-GO/p-Si Schottky diode structure has an orientation (100) and a resistivity of $1\text{--}20\ \Omega\cdot\text{cm}$, and $525\ \mu\text{m}$ thickness. Before preparing the diode structure, a cleaning procedure was applied to remove the inorganic and the organic impurities. using chloroform (CHCl_3), acetone ($\text{C}_3\text{H}_6\text{O}$), and methanol ($\text{C}_2\text{H}_6\text{O}$) in an ultrasonic cleaner for 5 min, respectively. To remove the oxide layer formed on the wafer, it was kept in $\text{HF}:\text{H}_2\text{O}$ (1:10) solution for 1 min and rinsed with distilled water.

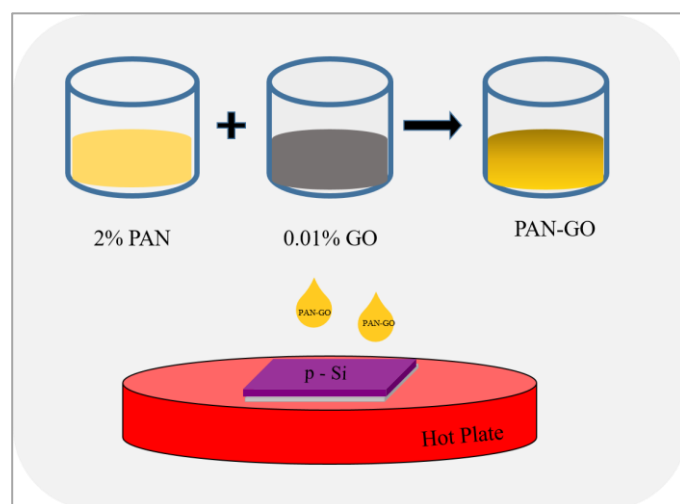


Figure 1. Experimental procedure of coating.

After cleaning, aluminum was deposited on the back of the p-Si to form ohmic contact using a thermal evaporation system under 10^{-6} Torr pressure. For the PAN-GO solution to be used as an interface layer, 2% by weight of PAN in powder form was dissolved in dimethylformamide ($\text{HCON}(\text{CH}_3)_2$) by stirring on a magnetic stirrer for 24 h. 0.01% by weight GO nanopowder was mixed in dimethylformamide for 3 h with a magnetic stirrer, then homogeneously dispersed in an ultrasonic cleaner for 1 h (Figure 1). These prepared solutions were mixed and the PAN-GO solution became ready. p-Si was placed on the hot plate at $45\ ^\circ\text{C}$. The solution was dropped onto the surface, and allowed to dry. Finally, aluminum was deposited by thermal evaporation as a rectifier contact. A schematic representation of the Schottky diode structure prepared as Al/PAN-GO/p-Si/Al is shown in Figure 2. Current-voltage characteristics were measured using a Keithley 4200 Sourcemeter with $0.01\ \text{V}$ step $\pm 4\ \text{V}$ bias range in the dark at room temperature.

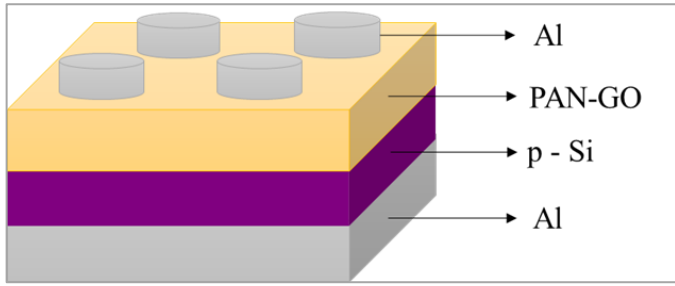


Figure 2. The schematic representation of the Al/PAN-GO/p-Si/Si/Al.

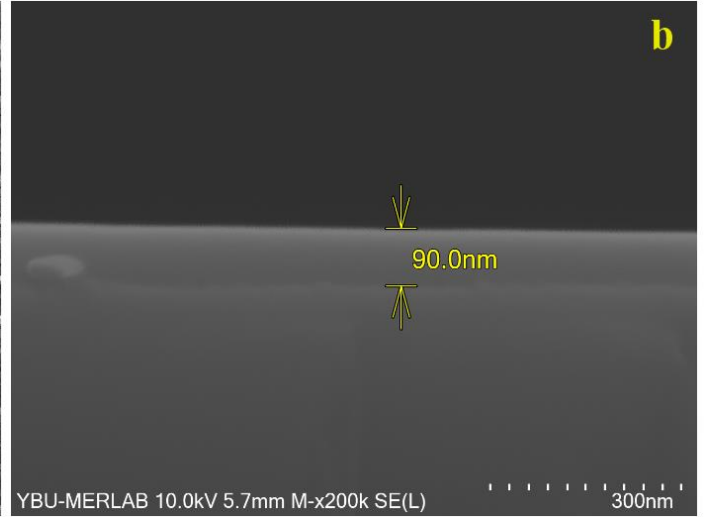
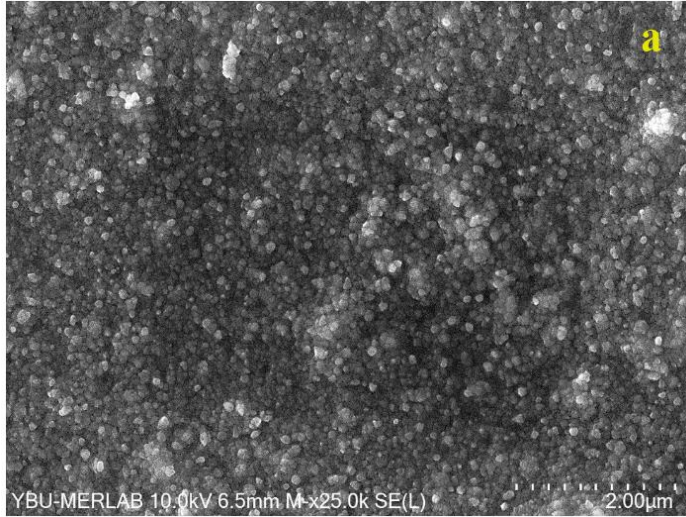


Figure 3. SEM images of (a) surface morphology (b) cross-section of Al/PAN-GO/p-Si/Al diode.

The electrical parameters of the Al/PAN-GO/p-Si/Al diode were calculated using the semi-logarithmic I - V graph given in Figure 4. As can be seen in Figure 4, the diode exhibited excellent rectifying behavior with a rectification ratio of 10^6 at ± 4 V. Due to this rectifying property of Al/PAN-GO/p-Si/Al diodes, the charge carriers follow the TE theory (Kaplan et al., 2021; Berktaş et al., 2022). Thus, according to TE theory, Al/PAN-GO/p-Si/Al diodes current-voltage equation in reverse and forward bias can be defined by the Eq. (1) and Eq. (2) [Rhoderick & Williams, 1988; Iwai et al., 2013; Kaplan et al., 2021; Şahin et al., 2021; Tezcan et al., 2021].

$$I = I_0 \exp\left(\frac{qV}{nkT}\right) \left[1 - \exp\left(-\frac{qV}{kT}\right)\right] \quad (1)$$

where,

$$I_0 = AA^*T^2 \exp\left[-\frac{q\Phi_B}{kT}\right] \quad (2)$$

where, q is the charge of electron; k is the Boltzmann constant; T is the absolute temperature in Kelvin; A is the diode area; A^* is the Richardson constant ($32 \text{ A/cm}^2\text{K}^2$) for p-Si (Yuksel et al., 2013; Luongo et al., 2018; Çaldıran, 2021). The I_0 value is used to determine the Φ_B of the Schottky diode, and the I_0 value is determined from the point where intercept the axis at $V=0$ in the $\ln I$ - V graph. The Φ_B and n are given in Eq. (3) and Eq. (4).

Results and Discussion

SEM images of PAN-GO grown on p-Si substrates are shown in Figure 3. As shown in Figure 3a, the PAN-GO film exhibits a uniformly distribution on p-Si substrate. It is seen in Figure 3b that the film thickness is around 90 nm.

$$\Phi_B = \frac{kT}{q} \ln\left(\frac{AA^*T^2}{I_0}\right) \quad (3)$$

$$n = \frac{q}{kT} \left(\frac{dV}{d(\ln I)}\right) \quad (4)$$

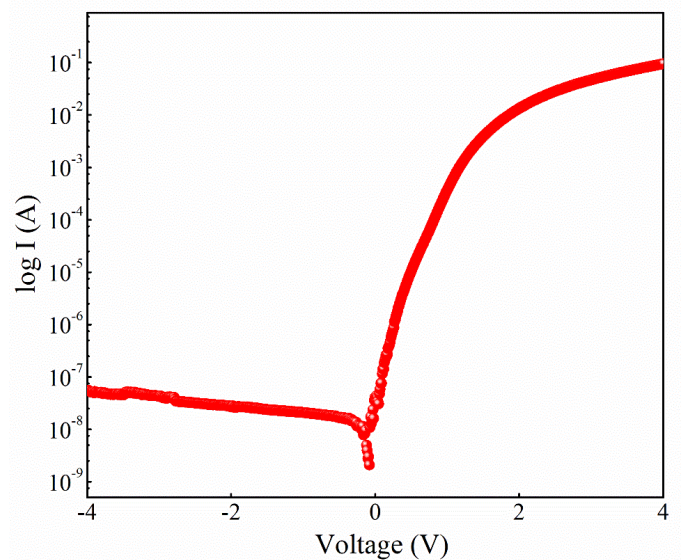


Figure 4. Current-voltage characteristics of Al/PAN-GO/p-Si/Al Schottky diode in dark at room temperature.

As can be seen from Figure 4, in the dark, characteristics of the produced Al/PAN-GO/p-Si/Al Schottky diode showed good rectification behavior. Using Eq. (3) and Eq. (4), n , Φ_B , and I_0 values were calculated and given in Table 1. n and Φ_B values were found as 2.078 and 0.767 eV, respectively. The value of n greater than 1 can be attributed to the inhomogeneity of the interface states, the presence of a thin interface natural oxide layer between the metal and the semiconductor, the series resistance, and the barrier at the metal-semiconductor interface (Batrır et al., 2018; Koca et al., 2021). Akin et al. (2022) have been introduced the electrical parameters of Al/p-Si and Al/Al₂O₃:PVP/p-Si Schottky diodes. They reported that the barrier height values are 0.638 eV and 0.735 eV for Al/p-Si and Al/Al₂O₃:PVP/p-Si diode, respectively. Hosseini et al. (2022) have been introduced the electrical parameters of Al/p-Si and Al/CdS-PVP/p-Si Schottky diodes. They reported that the barrier height values are 0.59 eV and 0.69 eV for Al/p-Si and Al/CdS-PVP/p-Si diode, respectively. When these values are compared with the barrier height of 0.767 eV calculated for the Al/PAN-GO/p-Si MPS diode, PAN-GO interfacial layer modified the value of barrier height.

The series resistance and barrier height values were evaluated using the Norde method. These functions are defined by considering voltages greater than $3kT/q$. In this method, metal-semiconductor contacts are assumed to be ideal. It is possible to calculate Φ_B and R_s values for non-ideal situations using the Bohlin's modified Norde method (Missoum et al., 2016; Nawar et al., 2020; Çaldıran, 2021). The modified Norde function is defined by Eq. (5);

$$F(V) = \frac{V}{\gamma} - \frac{kT}{q} \ln \left[\frac{I(V)}{A A^* T^2} \right] \quad (5)$$

Where, $I(V)$ is the current; γ is the first integer greater than n . The Φ_B of the Schottky diode can be determined using the plot of $F(V)$ - V and Eq. (6).

$$\Phi_B = F(V_{min}) + \frac{V_{min}}{\gamma} - \frac{kT}{q} \quad (6)$$

where, $F(V_{min})$ is the minimum value of $F(V)$ and V_{min} is the minimum voltage the of the $F(V)$ - V curve. The series resistance (R_s) of the Schottky diode is determined using Eq. (7). I_{min} and V_{min} values are at the minimum point of the $F(V)$ - V plot.

$$R_s = \frac{(\gamma-n)kT}{qI_{min}} \quad (7)$$

The graph of $F(V)$ - V for the Al/PAN-GO/p-Si/Al Schottky diode is shown in Figure 5. The R_s and Φ_B values calculated according to the Norde method are shown in Table 1. The R_s and Φ_B values are 42 k Ω and 0.761 eV, respectively.

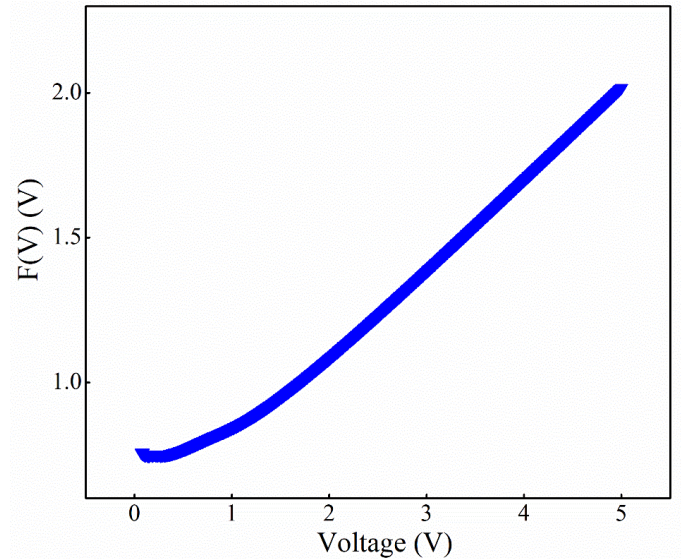


Figure 5. Plot of $F(V)$ - V for Al/PAN-GO/p-Si/Al diode.

The R_s values obtained by the Norde method in MPS type Schottky diodes are in the order of k Ω (Akin et al., 2022; Altındal et al., 2022; Hosseini et al., 2022). The reason for this is that the method allows to calculate the series resistance at low voltages. On the contrary, in diodes, the series resistance region is formed at high voltages.

Table 1. Characteristic parameters of Al/PAN-GO/p-Si/Al diode obtained from I - V measurements.

I - V			Norde	
$I_0 \times 10^{-8}$ (A)	n	Φ_B (eV)	Φ_B (eV)	R_s (k Ω)
1.646	2.078	0.767	0.761	42

Voltage dependent capacitance characteristic of Al/PAN-GO/p-Si/Al diode at 1 MHz is given in Figure 6. Using the maximum accumulation capacitance value of 5.97×10^{-10} F and the geometric thickness of the PAN-GO thin film layer determined from SEM image, the dielectric constant value of PAN-GO was evaluated with Eq. (8).

$$C_i = \frac{\epsilon_0 \epsilon_x}{d_i} A \quad (8)$$

where, C_i is the maximum capacitance value in the accumulation region of the C - V measurement of the diode; ϵ_x is the dielectric constant of the PAN-GO thin film layer; ϵ_0 is the dielectric constant of vacuum (8.85×10^{-12} F/m); and A is the rectifier contact area. The dielectric constant value of PAN-GO was calculated as 1.4.

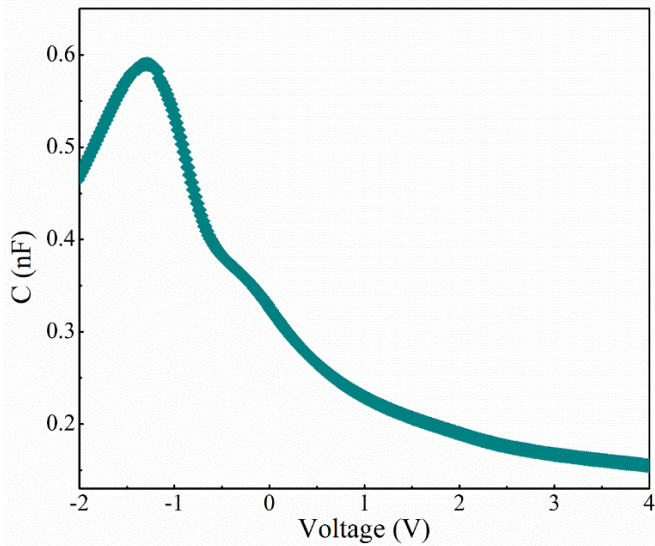


Figure 6. Plot of C - V for Al/PAN-GO/p-Si/Al diode.

Some parameters of Schottky diodes such as ideality factor and barrier height are effective in determining N_{ss} (Okutan et al., 2005; Akin et al., 2022; Karataş & Yumuk, 2022; Sevgili et al., 2022). The relationship between N_{ss} and n for a p-type semiconductor are expressed by Rhoderick (1988) as Eq. (9).

$$N_{ss}(V) = \frac{1}{q} \left[\frac{\epsilon_i}{\delta_i} (n(V) - 1) - \frac{\epsilon_s}{W_D} \right] \quad (9)$$

In Eq. (9), ϵ_s and ϵ_i are the dielectric constant of the semiconductor and interface, respectively. The thin film layer thickness is δ_i and the depletion zone width is W_D . In a p-type semiconductor, the relationship of the valence band limit energy (E_v) of the semiconductor with the energy of the interface state density (E_{ss}) is expressed as Eq. (10):

$$E_{ss} - E_v = q(\Phi_e - V); \Phi_e = \Phi_{B0} + \beta V = \Phi_{B0} + \left(1 - \frac{1}{n(V)}\right) V \quad (10)$$

where, Φ_e is the effective barrier height and q is the electron charge.

Figure 7 shows the N_{ss} profile of the Al/PAN-GO/p-Si/Al diode derived from the forward bias I - V . The N_{ss} values of the diode are $9.5 \times 10^{11} \text{ eV}^{-1} \text{ cm}^{-2}$ for $0.35 - E_v$ eV and $1.03 \times 10^{11} \text{ eV}^{-1} \text{ cm}^{-2}$ for $0.74 - E_v$ eV. Figure 7 demonstrates a decrease in N_{ss} attributable to the discharge and charge of the interface states due to increasing voltage.

Both Akin et al. (2022) and Hosseini et al. (2022) determined the interfacial state density distribution in the energy band gap at the order of $10^{13} \text{ eV}^{-1} \text{ cm}^{-2}$. Compared to their N_{ss} value, the obtained value of $10^{11} \text{ eV}^{-1} \text{ cm}^{-2}$ for the

interfacial state density distribution of Al/PAN-GO/p-Si MPS diode is better.

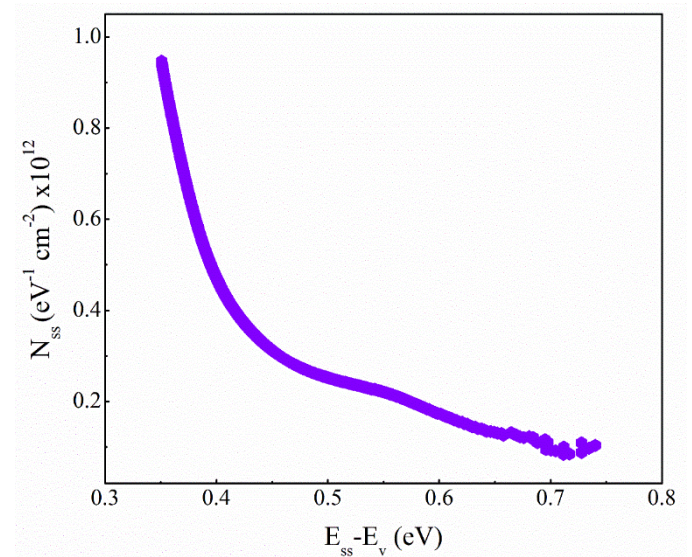


Figure 7. The energy-dependent distribution of the N_{ss} obtained from the forward-bias I - V data for the Al/PAN-GO/p-Si/Al diode.

Conclusion

In the presented article, the Al/PAN-GO/p-Si Schottky diode was prepared by a drop casting method. The I - V measurement of Al/PAN-GO/p-Si diode was performed in dark at 300 K. The morphology of the prepared diode was examined by SEM. Because of SEM measurement, the thickness of the PAN-GO film was calculated as 90 nm. A good rectification behavior with low reverse leakage current is achieved for the Al/PAN-GO/p-Si Schottky diode. The diode parameters such as the ideality factor, barrier height and series resistance are calculated for the prepared diode by I - V and Norde method. The effects of N_{ss} on I - V measurements were also examined. The energy-dependent profiles of N_{ss} was obtained from the I - V method. The N_{ss} of the diode has ranged from $29.5 \times 10^{11} \text{ eV}^{-1} \text{ cm}^{-2}$ for $0.35 - E_v$ eV and $1.03 \times 10^{11} \text{ eV}^{-1} \text{ cm}^{-2}$ for $0.74 - E_v$ eV. The experimental observations show that the thermionic emission is the dominant conduction mechanism in the forward bias region of the Al/PAN-GO/p-Si Schottky diode.

Conflict of Interest

The authors declare that they have no conflict of interest.

References

- Aftab, S., Samiya, M., Liao, W., Iqbal, M. W., Ishfaq, M., Ramachandraiah, K., Ajmal, H. M. S., Haque, H. M. U., Yousuf, S., Ahmed, Z., Usman Khan, M., Rehman, A. U., & Iqbal, M. Z. (2021). Switching photodiodes based on (2D/3D) PdSe₂/Si heterojunctions with a broadband spectral response. *Journal of Materials Chemistry C*, 9(11), 3998-4007. <https://doi.org/10.1039/d0tc05894g>
- Akin, B., Farazin, J., Altındal, Ş., & Azizian-Kalandaragh, Y. (2022). A comparison electric-dielectric features of Al/p-Si (MS) and Al/ (Al₂O₃:PVP)/p-Si (MPS) structures using voltage-current (V-I) and frequency-impedance (f-Z) measurements. *Journal of Materials Science: Materials in Electronics*, 33(27), 21963-21975. <https://doi.org/10.1007/s10854-022-08984-2>
- Al-Ahmadi, N. A. (2020). Metal oxide semiconductor-based Schottky diodes: A review of recent advances. *Materials Research Express*, 7(3) 032001. <https://doi.org/10.1088/2053-1591/ab7a60>
- Aldirmaz, E., Guler, M., Guler, E., Dere, A., Tataroğlu, A., Al-Sehemi, A. G., Al-Ghamdi, A. A., & Yakuphanoglu, F. (2018). A shape memory alloy based on photodiode for optoelectronic applications. *Journal of Alloys and Compounds*, 743, 227-233. <https://doi.org/10.1016/j.jallcom.2018.01.380>
- Aldirmaz, E., Güler, M., & Güler, E. (2022). Illumination intensities effect on electronic properties of Fe-Ni-Mn/p-Si Schottky diode. *Journal of Materials Science: Materials in Electronics*, 33(7), 4132-4144. <https://doi.org/10.1007/s10854-021-07609-4>
- Altındal, Ş., Azizian-Kalandaragh, Y., Ulusoy, M., & Pirgholi-Givi, G. (2022). The illumination effects on the current conduction mechanisms of the Au/(Er₂O₃:PVC)/n-Si (MPS) Schottky diodes. *Journal of Applied Polymer Science*, 139(27), 1-12. <https://doi.org/10.1002/app.52497>
- Batır, G. G., Arik, M., Caldıran, Z., Turut, A., & Aydoğan, S. (2018). Synthesis and characterization of reduced graphene oxide/rhodamine 101 (rGO-Rh101) nanocomposites and their heterojunction performance in rGO-Rh101/p-Si device configuration. *Journal of Electronic Materials*, 47(1), 329-336. <https://doi.org/10.1007/s11664-017-5758-4>
- Berktaş, Z., Yıldız, M., Seven, E., Öz Orhan, E., & Altındal, Ş. (2022). PEI N-doped graphene quantum dots/p-type silicon Schottky diode. *FlatChem*, 36, 100436. <https://doi.org/10.1016/j.flatc.2022.100436>
- Bohlin, K. E. (1986). Generalized Norde plot including determination of the ideality factor. *Journal of Applied Physics*, 60(3), 1223-1224. <https://doi.org/10.1063/1.337372>
- Çaldıran, Z. (2021). Modification of Schottky barrier height using an inorganic compound interface layer for various contact metals in the metal/p-Si device structure. *Journal of Alloys and Compounds*, 865, 158856. <https://doi.org/10.1016/j.jallcom.2021.158856>
- Eswaran, M., Chokkiah, B., Pandit, S., Rahimi, S., Dhanusuraman, R., Aleem, M., & Mijakovic, I. (2022). A road map toward field-effect transistor biosensor technology for early stage cancer detection. *Small Methods*, 6(10). <https://doi.org/10.1002/smt.202200809>
- Ferrag, C., Noroozifar, M., Modarresi-Alam, A. R., & Kerman, K. (2022). Graphene oxide hydrogel electrolyte for improving the performance of electropolymerized polyaniline solar cells. *Journal of Power Sources*, 542, 231796. <https://doi.org/10.1016/j.jpowsour.2022.231796>
- Gholami, S., Hajghassem, H., & Erfanian, A. R. (2009). The gaussian distribution of inhomogeneous barrier heights in PtSi/p-Si Schottky diodes. *IEICE Electronics Express*, 6(13), 972-978. <https://doi.org/10.1587/elex.6.972>
- Güllü, Ö., & Türüt, A. (2010). Electrical analysis of organic dye-based MIS Schottky contacts. *Microelectronic Engineering*, 87(12), 2482-2487. <https://doi.org/10.1016/j.mee.2010.05.004>
- Gupta, R. K., Ghosh, K., & Kahol, P. K. (2009). Effect of temperature on current-voltage characteristics of Cu₂O/p-Si Schottky diode. *Physica E: Low-Dimensional Systems and Nanostructures*, 41(5), 876-878. <https://doi.org/10.1016/j.physe.2008.12.025>
- Hosseini, Z., Azizian-Kalandaragh, Y., Sobhanian, S., Pirgholi-Givi, G., & Kouhi, M. (2022). Comparison of capacitance-frequency and current-voltage characteristics of Al/CdS-PVP/p-Si and Al/p-Si structures. *Physica B: Condensed Matter*, 640, 413836. <https://doi.org/10.1016/j.physb.2022.413836>
- Hue, N. T., Wu, Q., Liu, W., Bu, X., Wu, H., Wang, C., Li, X., & Wang, X. (2020). Graphene oxide/graphene hybrid film with ultrahigh ammonia sensing performance. *Nanotechnology*, 32(11), 115501. <https://doi.org/10.1088/1361-6528/abd05a>
- Iwai, H., Sze, S. M., Taur, Y., & Wong, H. (2013). MOSFETs. In J. N. Burghartz (Ed.), *Guide to state-of-the-art electron devices* (pp. 21-36). Wiley. <https://doi.org/10.1002/9781118517543.ch2>
- Jaworski, S., Sawosz, E., Kutwin, M., Wierzbicki, M., Hinzmann, M., Grodzik, M., Winnicka, A., Lipińska, L., Włodyga, K., & Chwalibog, A. (2015). *In vitro* and *in vivo* effects of graphene oxide and reduced graphene oxide on glioblastoma. *International Journal of Nanomedicine*, 10, 1585-1596. <https://doi.org/10.2147/IJN.S77591>
- Kang, B., Cai, Y., & Wang, L. (2016). Improvement of external quantum efficiency of silicide Schottky-barrier detectors in the 3 to 5 μm waveband with subwavelength-grating incident plane. *Optical Engineering*, 55(4), 047103. <https://doi.org/10.1117/1.oe.55.4.047103>
- Kaplan, N., Taşçı, E., Emrullahoğlu, M., Gökce, H., Tuğluoğlu, N., & Eymur, S. (2021). Analysis of illumination dependent electrical characteristics of α-styryl

- substituted BODIPY dye-based hybrid heterojunction. *Journal of Materials Science: Materials in Electronics*, 32(12), 16738-16747. <https://doi.org/10.1007/s10854-021-06231-8>
- Karataş, Ş., & Yumuk, M. (2022). Electrical characteristics of Al/(GO:PTCDA)/p-type Si structure under dark and light illumination: photovoltaic properties at 40 mW cm⁻². *Journal of Materials Science: Materials in Electronics*, 33(14), 10800-10813. <https://doi.org/10.1007/s10854-022-08061-8>
- Kedambaimoole, V., Kumar, N., Shirhatti, V., Nuthalapati, S., Nayak, M. M., & Konandur, R. (2020). Electric spark induced instantaneous and selective reduction of graphene oxide on textile for wearable electronics. *ACS Applied Materials and Interfaces*, 12(13), 15527-15537. <https://doi.org/10.1021/acsami.9b22497>
- Koca, M., Yilmaz, M., Ekinici, D., & Aydoğan. (2021). Light sensitive properties and temperature-dependent electrical performance of n-TiO₂/p-Si anisotype heterojunction electrochemically formed TiO₂ on p-Si. *Journal of Electronic Materials*, 50(9), 5184-5195. <https://doi.org/10.1007/s11664-021-09040-1>
- Kumar, M., Bhati, V. S., & Kumar, M. (2017). Effect of Schottky barrier height on hydrogen gas sensitivity of metal/TiO₂ nanoplates. *International Journal of Hydrogen Energy*, 42(34), 22082-22089. <https://doi.org/10.1016/j.ijhydene.2017.07.144>
- Lu, A., Kiefer, A., Schmidt, W., & Schüth, F. (2004). Synthesis of polyacrylonitrile-based ordered mesoporous carbon with tunable pore structures. *Chemistry of Materials*, 16(1), 100-103. <https://doi.org/10.1021/cm031095h>
- Luongo, G., Di Bartolomeo, A., Giubileo, F., Chavarin, C. A., & Wenger, C. (2018). Electronic properties of graphene/p-silicon Schottky junction. *Journal of Physics D: Applied Physics*, 51(25). <https://doi.org/10.1088/1361-6463/aac562>
- Lv, L., Hui, B., Zhang, X., Zou, Y., & Yang, D. (2023). Lamellar agarose/graphene oxide gel polymer electrolyte network for all-solid-state supercapacitor. *Chemical Engineering Journal*, 452, 139443. <https://doi.org/10.1016/j.cej.2022.139443>
- Mahala, P., Patel, M., Gupta, N., Kim, J., & Lee, B. H. (2018). Schottky junction interfacial properties at high temperature: A case of AgNWs embedded metal oxide/p-Si. *Physica B: Condensed Matter*, 537, 228-235. <https://doi.org/10.1016/j.physb.2018.02.010>
- Missoum, I., Ocak, Y. S., Benhaliliba, M., Benouis, C. E., & Chaker, A. (2016). Microelectronic properties of organic Schottky diodes based on MgPc for solar cell applications. *Synthetic Metals*, 214, 76-81. <https://doi.org/10.1016/j.synthmet.2016.01.004>
- Muazim, K., & Hussain, Z. (2017). Graphene oxide - A platform towards theranostics. *Materials Science and Engineering C*, 76, 1274-1288. <https://doi.org/10.1016/j.msec.2017.02.121>
- Nataraj, S. K., Yang, K. S., & Aminabhavi, T. M. (2012). Polyacrylonitrile-based nanofibers - A state-of-the-art review. *Progress in Polymer Science (Oxford)*, 37(3), 487-513. <https://doi.org/10.1016/j.progpolymsci.2011.07.001>
- Nawar, A. M., Abd-Elsalam, M., El-Mahalawy, A. M., & El-Nahass, M. M. (2020). Analyzed electrical performance and induced interface passivation of fabricated Al/NTCDA/p-Si MIS-Schottky heterojunction. *Applied Physics A: Materials Science and Processing*, 126, 113. <https://doi.org/10.1007/s00339-020-3289-y>
- Norde, H. (1979). A modified forward I-V plot for Schottky diodes with high series resistance. *Journal of Applied Physics*, 50(7), 5052-5053. <https://doi.org/10.1063/1.325607>
- Okutan, M., Basaran, E., & Yakuphanoglu, F. (2005). Electronic and interface state density distribution properties of Ag/p-Si Schottky diode. *Applied Surface Science*, 252(5), 1966-1973. <https://doi.org/10.1016/j.apsusc.2005.03.155>
- Rhoderick, E. H., & Williams, R. H. (1988). *Metal-semiconductor contacts*. Clarendon Press.
- Şahin, M. F., Taşcı, E., Emrullahoğlu, M., Gökce, H., Tuğluoğlu, N., & Eymur, S. (2021). Electrical, photodiode, and DFT studies of newly synthesized π -conjugated BODIPY dye-based Au/BOD-Dim/n-Si device. *Physica B: Condensed Matter*, 614, 413029. <https://doi.org/10.1016/j.physb.2021.413029>
- Saloma, E., Alcántara, S., Hernández-Como, N., Villanueva-Cab, J., Chavez, M., Pérez-Luna, G., & Alvarado, J. (2020). Photoelectric effect on an Al/SiO₂/p-Si Schottky diode structure. *Materials Research Express*, 7(10), 105902. <https://doi.org/10.1088/2053-1591/abbc40>
- Saufi, S. M., & Ismail, A. F. (2002). Development and characterization of polyacrylonitrile (PAN) based carbon hollow fiber membrane. *Songklanakarin Journal of Science and Technology*, 24, 843-854.
- Sevgili, Ö., Orak, İ., & Tiras, K. S. (2022). The examination of the electrical properties of Al/Mg₂Si/p-Si Schottky diodes with an ecofriendly interfacial layer depending on temperature and frequency. *Physica E: Low-Dimensional Systems and Nanostructures*, 144, 115380. <https://doi.org/10.1016/j.physe.2022.115380>
- Strimaitis, J., Danquah, S. A., Denize, C. F., Pradhan, S. K., & Bahoura, M. (2022). The effects of graphene oxide and reduced graphene oxide conductive additives on activated carbon supercapacitors. *Processes*, 10(11), 2190. <https://doi.org/10.3390/pr10112190>
- Suk, J. W., Piner, R. D., An, J., & Ruoff, R. S. (2010). Mechanical properties of monolayer graphene oxide. *ACS Nano*, 4(11), 6557-6564. <https://doi.org/10.1021/NN101781V>
- Sun, J., Oh, S., Choi, Y., Seo, S., Oh, M. J., Lee, M., Lee, W. B., Yoo, P. J., Cho, J. H., & Park, J. H. (2018). Optoelectronic synapse based on IGZO-alkylated graphene oxide hybrid

- structure. *Advanced Functional Materials*, 28(47), 1-9. <https://doi.org/10.1002/adfm.201804397>
- Tatar, B., Bulgurcuoğlu, A. E., Gökdemir, P., Aydoğan, P., Yilmazer, D., Özdemir, O., & Kutlu, K. (2009). Electrical and photovoltaic properties of Cr/Si Schottky diodes. *International Journal of Hydrogen Energy*, 34(12), 5208-5212. <https://doi.org/10.1016/J.IJHYDENE.2008.10.040>
- Tezcan, A. O., Eymur, S., Taşcı, E., Emrullahoğlu, M., & Tuğluoğlu, N. (2021). Investigation of electrical and photovoltaic properties of Au/n-Si Schottky diode with BOD-Z-EN interlayer. *Journal of Materials Science: Materials in Electronics*, 32(9), 12513-12520. <https://doi.org/10.1007/s10854-021-05886-7>
- Tian, J., Wu, S., Yin, X., & Wu, W. (2019). Novel preparation of hydrophilic graphene/graphene oxide nanosheets for supercapacitor electrode. *Applied Surface Science*, 496, 143696. <https://doi.org/10.1016/J.APSUSC.2019.143696>
- Vacchi, I. A., Ménard-Moyon, C., & Bianco, A. (2017). Chemical functionalization of graphene family members. *Physical Sciences Reviews*, 2(1), 1-18. <https://doi.org/10.1515/psr-2016-0103>
- Wang, W. S., Ho, C., & Chuang, T. M. (1998). High-performance IR detectors fabricated by PtSi on p-Si substrate. *Infrared Detectors and Focal Plane Arrays V*, 3379, 333. <https://doi.org/10.1117/12.317600>
- Yıldırım, M., Kocyigit, A., Torlak, Y., Yenel, E., Hussaini, A. A., & Kuş, M. (2022). Electrical behaviors of the Co- and Ni-based POMs interlayered Schottky photodetector devices. *Advanced Materials Interfaces*, 9(18), 1-10. <https://doi.org/10.1002/admi.202102304>
- Yuksel, O. F., Tuğluoğlu, N., Gulveren, B., Şafak, H., & Kuş, M. (2013). Electrical properties of Au/perylene-monoimide/p-Si Schottky diode. *Journal of Alloys and Compounds*, 577, 30-36. <https://doi.org/10.1016/j.jallcom.2013.04.157>
- Zhang, D., Fu, C., Xu, J., Zhao, C., Gao, J., Liu, Y., Li, M., Li, J., Wang, W., Chen, D., Ye, T., Wu, D., & Luo, J. (2021). NiSi/p⁺-Si(n⁺-Si)/n-Si(p-Si) diodes with dopant segregation (DS): p-n or Schottky junctions? *IEEE Transactions on Electron Devices*, 68(6), 2886-2891. <https://doi.org/10.1109/TED.2021.3075199>